Antimicrobial Resistance

Deutsche Ausgabe: DOI: 10.1002/ange.201505700
Internationale Ausgabe: DOI: 10.1002/anie.201505700

Aromatic Esters of Bicyclic Amines as Antimicrobials against *Streptococcus pneumoniae*

María de Gracia Retamosa, Roberto Díez-Martínez, Beatriz Maestro, Esther García-Fernández, Bas de Waal, E. W. Meijer, Pedro García, and Jesús M. Sanz**

Abstract: *A double approach was followed in the search of novel inhibitors of the surface choline-binding proteins (CBPs) of Streptococcus pneumoniae (pneumococcus) with antimicrobial properties. First, a library of 49 rationally-designed esters of alkyl amines was screened for their specific binding to CBPs. The best binders, being esters of bicyclic amines (EBAs), were then tested for their in vitro effect on pneumococcal growth and morphology. Second, the efficiency of EBA-induced CBP inhibition was enhanced about 45 000-fold by multivalency effects upon synthesizing a poly(propylene imine) dendrimer containing eight copies of an atropine derivative. Both approaches led to compounds that arrest bacterial growth, dramatically decrease cell viability, and exhibit a protection effect in animal disease models, demonstrating that the pneumococcal CBPs are adequate targets for the discovery of novel antimicrobials that overcome the currently increasing antimicrobial resistance issues.*

Antimicrobial resistance (AMR) to traditional antibiotics constitutes a first-order problem in current healthcare, and may lead to a post-antibiotic era in which many common infections would be unable to be effectively treated.[1]

Streptococcus pneumoniae is a major causative agent of pneumonia, meningitis, and otitis media worldwide, with an estimated 1.6 million deaths per year.[2] AMR has had a serious impact on the pneumococcal infections, which are increasingly difficult to treat owing to the emergence of resistant strains.[1,2] Therefore, prompt actions to attack this problem are needed, including the search for novel compounds directed to new targets common to most pneumococcal isolates.

Choline-binding proteins (CBPs) are a family of bacterial surface-exposed polypeptides that play key cellular roles, such as adhesion to the host, separation of daughter cells, and toxin release.[3] CBPs are organized into a functional module and a choline-binding module (CBM), the latter of which is responsible for the attachment to the choline residues present in teichoic and lipoteichoic acids of the bacterial cell wall.[4] CBMs contain 20-amino acid tandem repetitions known as choline-binding repeats (CBRs), which are β-hairpin-loop structures rich in aromatic residues that bind choline through hydrophobic and cation–π interactions.[4]

Several choline analogues,[5] and in particular esters of bicyclic amines (EBAs) such as atropine and ipratropium,[5b] are efficient inhibitors of CBPs. They arrest pneumococcal growth in vitro and highly decrease cell viability (> 90 %), although at concentrations far from therapeutically acceptable. On the other hand, the multivalent display of choline in poly(propylene imine) (PPI) dendrimers exponentially increases its affinity for CBPs,[6] causing inhibition of daughter cell separation after division and favoring phagocytosis by microglial cells.[7] The aim of our work was the improvement of EBA druggability by enhancing their binding to CBPs, following two complementary approaches: the rational design and assay of new EBA derivatives, and the multivalent display of EBAs on the surface of a PPI dendrimer.

Analysis of crystalline complexes between the pneumococcal CBP CbpF and atropine[8] points, as the major determinant for stronger EBA binding, to the simultaneous involvement of tryptophan residues in the binding site with the ammonium group in the ligand (through cation–π forces), and with its aromatic moiety (involving T-shaped π–π stacking). Therefore, we synthetized a library of 49 derivatives of choline, atropine, and ipratropium, paying special attention to the diversity in the number of aromatic rings and their spatial disposition (Supporting Information, Scheme S1). Relevant compounds displaying the lowest minimal bacterial inhibitory concentrations (MICs) are shown in Scheme 1 a. For ease of synthesis, ipratropium derivatives contain an ethyl N-substituent instead of an isopropyl group.

To screen the library, we first checked the effect of these compounds on the fluorescence anisotropy of the C-LytA-GFP hybrid protein, which contains the CBM of the pneumococcal LytA amidase (C-LytA) fused to the green fluorescent protein (GFP). Previous reports demonstrated that millimolar concentrations of choline induce C-LytA dimerization,

[*] Dr. M. G. Retamosa,[$] [+] Dr. B. Maestro, Prof. J. M. Sanz
Instituto de Biología Molecular y Celular,
Universidad Miguel Hernández
Avda. de la Universidad s/n, 03202 Elche (Spain)
E-mail: jmsanz@umh.es
Dr. R. Díez-Martínez,[+] Dr. E. García-Fernández, Dr. P. García
Departamento de Microbiología Molecular y
Biología de las Infecciones,
Centro de Investigaciones Biológicas (CSIC) and
CIBER de Enfermedades Respiratorias (CibeRes)
Ramiro de Maeztu, 9, 28040 Madrid (Spain)
E-mail: pgarcia@cib.csic.es
B. de Waal, Prof. E. W. Meijer
Institute for Complex Molecular Systems,
Eindhoven University of Technology
5600MB Eindhoven (The Netherlands)
[$] Present address: Universidad del País Vasco (UPV/EHU) and Donostia International Physics Center (DIPC) (Spain)
[+] These authors contributed equally to this work.

Supporting information for this article is available on the WWW under http://dx.doi.org/10.1002/anie.201505700.

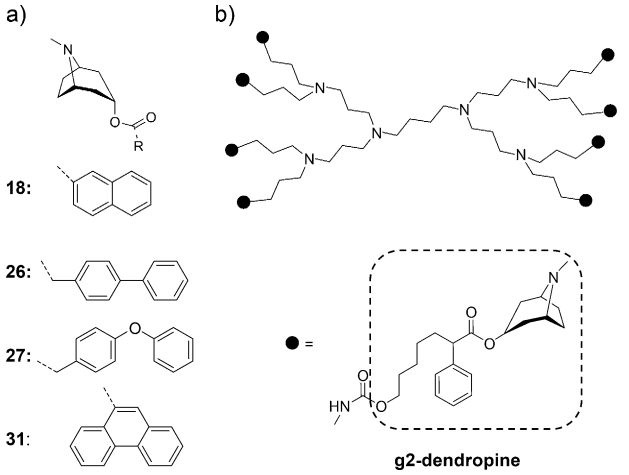

Scheme 1. Chemical structures of the most representative compounds used in this study. a) Esters of bicyclic amines with the lowest minimal inhibitory concentrations on D39 strain. b) Second generation PPI dendrimer functionalized with **2b** (g2-dendropine). Dashed box contains the **2b** compound structure.

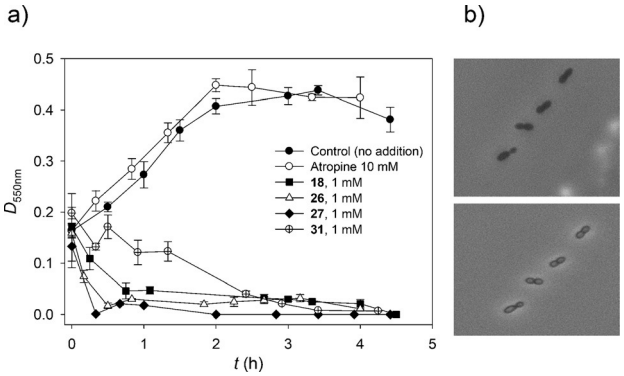

Figure 1. Effect of selected EBAs on R6 pneumococcal growth. a) Attenuation of liquid cultures. Error bars represent the standard deviation (s.d.) of duplicates. b) Phase-contrast micrographs of bacteria before (upper photograph) and 45 min after being challenged with **31** (lower photograph).

Table 1: Effect of selected EBAs on in vitro R6 and D39 pneumococcal cultures.

Compound	Decrease in attenuance at 550 nm [%][a,b]		Cell viability [%][c] (±0.001)[d]		Minimal inhibitory concentration (MIC) [μM]	
	R6	D39	R6	D39	R6	D39
18	>99	95±4[d]	0.003	0.005	180	180
26	>99	90±5	<0.001	0.040	90	90
27	>99	>99	<0.001	<0.001	90	90
31	>99	55±4	<0.001*	<0.001*	22	22

[a] Relative to the D_{550nm} value at the zero time. [b] [Compound] = 1 mM. [c] [Compound] = 0.5 mM except (*), 0.1 mM. [d] Standard deviation of duplicates.

bringing together the GFP moieties and inducing a decrease in fluorescence anisotropy as a result of energy transfer.[6a]

Using this assay, 1 mM solutions of most EBAs induced a higher decrease in anisotropy than choline, atropine, or ipratropium (Supporting Information, Figure S1), leading in some cases to visible aggregation, and suggesting stronger binding to the C-LytA module. Moreover, those molecules with two or three aromatic rings display the most remarkable results (Supporting Information, Figure S1), which can be attributed to an enhanced π–π interaction with the aromatic residues in the binding sites.[8] Therefore, we focused on those compounds that induced an anisotropy decrease equal or greater than 20%, or resulted in protein precipitation, as well as appearing synthetically accessible and water-soluble (Supporting Information, Table S2).

We then assayed the selected EBAs on bacterial cultures of both non-capsulated (R6) and type-2 capsulated (D39) pneumococcal strains. Most of the EBAs tested, and especially those with the tertiary amine (see below), arrested cellular growth at 1 mM concentration, causing bacterial lysis in many cases (Figure 1, see Table 1 for select compounds; Supporting Information, Figures S2, S3, Table S2). It is worth noting that bacterial lysis was preceded by a change in cell appearance consisting of a "white" phenotype while the overall shape was conserved (Figure 1b; Supporting Information, Figure S4). In contrast, 10 mM atropine did not produce any detectable effect. Furthermore, cellular viability substantially decreased to various extents when the cultures were challenged with the EBAs (Table 1; Supporting Information, Table S2). This suggests that the stronger apparent binding of these molecules to the CBPs in vitro as compared to atropine or ipratropium (Supporting Information, Figure S1) is also translated into a more effective antimicrobial behavior.

The negative effect of EBAs on pneumococcal growth and viability is observed both in non-virulent, non-capsulated (R6) and in capsulated (D39) strains (Tables 1; Supporting Information, Figures S2, S3), although the antibacterial efficiency is somehow diminished in the latter. This is a strong indication that EBAs might be applied as antimicrobials to all virulent strains independent of their capsular type. MICs are in the micromolar range for both strains (Table 1; Supporting Information, Table S2). This represents a 2–3 magnitude-order improvement over the 1-ring starting compounds atropine and ipratropium, with MICs in the range of 12–15 mM.[5b] The most effective compounds, as defined by the lowest MIC on D39 and causing the highest decrease on cell viability at the lowest concentration, are **18**, **26**, **27**, and **31** (Scheme 1).

To evaluate the capacity of EBAs to specifically inhibit CBPs, the selected compounds were checked for in vitro inhibition of the LytA amidase (Table 2). These molecules diminished enzymatic activity at much lower concentrations than choline (IC_{50} = 9.1 mM) and atropine (IC_{50} = 4.5 mM). Remarkably, **31** evidenced the highest inhibition capacity (IC_{50} = 0.1 mM), representing a 45-fold improvement over atropine. On the other hand, simultaneous addition of **31** (final concentration = 0.1 mM) and excess choline (150 mM) to R6 and D39 cultures led to a substantial reduction of bacterial lysis concomitant with an increase in viability (Supporting Information, Table S3), indicating that high choline concentrations may partially revert EBA binding to CBPs.

Table 2: Inhibition of in vitro LytA cell wall lytic activity by selected compounds.

Compound	IC_{50}[a] [mM]
18	0.80 ± 0.05
26	0.20 ± 0.04
27	1.10 ± 0.05
31	0.10 ± 0.01
g2-dendropine	0.00010[b] ± 0.00001

[a] IC_{50}: [compound] required for 50% inhibition of enzymatic activity. [b] Concentration in atropine equivalents = 0.0008 mM.

The most efficient compounds both in terms of cell lysis and viability loss correspond (on an equal aromatic moiety) to tertiary, bicyclic amines (Supporting Information, Table S2). Non-bicyclic amines display diminished binding to C-LytA (Supporting Information, Figure S1), which can be ascribed to the lower ligand surface burial and decreased van der Waals interactions. In contrast, quaternary amines, though better binders in vitro (Supporting Information, Figure S1), show poorer results, probably owing to reduced availability in vivo.

To further investigate the molecular basis of EBA binding, we carried out a detailed C-LytA-GFP anisotropy-monitored titration with some representative compounds (Supporting Information, Figure S5). All of the molecules induced a sigmoidal transition. Addition of choline and atropine led to final anisotropy values of around 0.28, representing the formation of protein dimers.[6a] Nevertheless, most of the EBAs decreased the anisotropies to much lower values, suggesting a massive energy transfer between GFP moieties as a consequence of protein association and eventual precipitation. Such aggregates are EBA-specific as addition of an excess choline (150 mM) displaced the bound EBAs, resolubilizing the protein, and restoring the anisotropies to dimer values around 0.28 (data not shown). Next, we performed a docking simulation of the binding of **31**, the EBA displaying the highest inhibitory effect, to C-LytA. We then selected, among the most stable conformations, those with binding modes similar to experimental CbpF-atropine complexes, that is, displaying favorable T-shaped π–π interactions with the aromatic residues in the binding sites.[8] The bulky aromatic moiety of EBAs would generate extensive solvent-exposed non-polar patches that easily favor intermolecular aggregation (Supporting Information, Figure S6a, b).

The final oligomeric state at the end of the titration is undefined and certainly different among EBAs (Supporting Information, Figure S5). Therefore, binding curves were not subjected to thermodynamic analysis and, thus, we will refer to apparent affinities from this point on. To evaluate the relative binding strengths, we chose the minimal ligand concentration required to achieve an anisotropy value of 0.28 (representative of soluble dimers, as stated above) as a parameter of binding efficiency. A direct correlation between EBA apparent binding affinity and bacterial MICs was observed (Supporting Information, Figure S5b, Table S4), suggesting that fluorescence experiments constitute a suitable approach to explain the antimicrobial behavior of EBAs. To better characterize the binding, we also carried out surface plasmon resonance experiments that yielded poor signals, most probably owing to the low molecular weight of the ligands (data not shown). On the other hand, several representative EBAs were subjected to docking procedures using the C-LytA choline-binding site configured by repeats 4 and 5 (CBR4-5 site), and responsible for protein dimerization, as a target (Supporting Information, Figure S6 and Table S4).[9] These data, together with those shown in Figure S5 (Supporting Information), suggest that binding of EBAs depends on several factors, namely polarity, number and geometry of aromatic rings, and buried protein surface. Thus, the binding of three-ringed **30** and **31** could be most favored as they optimize these aspects (see the Supporting Information, Figure S5c). Their three adjacent aromatic rings configure an extensive interaction area (Supporting Information, Table S4) capable of establishing strong van der Waals contacts and T-shaped π-π interactions with the aromatic residues in the binding site. Moreover, the flatness of the aromatic system creates a smooth hydrophobic patch on the protein surface (Supporting Information, Figure S6b, c) that would eventually promote intermolecular aggregation in vitro. On the other hand, two-ringed compounds have a decreased binding strength as a consequence of the lack of an aromatic ring and a smaller burial surface (Supporting Information, Figure S5c). Within this group, those with non-adjacent rings (**26**, **27**, and **29**) show better interactions than naphthalene-derived compounds (**18** and **20**), because the former cover a higher protein surface, leading to enhanced aggregation (Supporting Information, Figure S5a). One exception is **25**, which, despite having separate rings, presents a relatively poor interaction with the protein as a consequence of its rough geometry (Supporting Information, Figures S5c and S6c).

Remarkably, heterocyclic two-ring compounds **21**, **22**, and **23** displayed only discrete changes in C-LytA-GFP anisotropy (Supporting Information, Figures S1 and S5a). Heterocycle polarity has been described to decrease the strength of T-shaped π–π interactions in favor of parallel displaced interactions,[10] and is also likely to decrease hydrophobic protein-protein associations. Accordingly, heterocyclic EBAs exert a limited antipneumococcal effect (Supporting Information, Figure S2 and Table S2).

To validate the bactericidal results of EBAs, we employed a zebrafish embryo model of infection.[11] The most appropriate bacterial challenge dose causing 50% mortality after 5 days was found to be 2.5×10^8 cfu mL^{-1} for pneumococcal strain D39, when administered by immersion. Seven hours after bacterial challenge, embryos were treated with a single dose containing different amounts of **31**, or phosphate buffer as control, and this operation was repeated for the first three days. Embryo survival was followed over 5 days and the results of three experiments were combined and represented as a Mantel–Cox curve (Figure 2). Rescue of the treated embryos was almost total, reaching 97.9% survival (47/48) at 2 μM **31**, and 93.7% (45/48) with 1 μM, indicating the great efficiency of **31** to protect zebrafish embryos from pneumococcal infection.

In vitro MICs of EBAs are in the micromolar range (Table S2). The best compound (**31**) shows a MIC of 22 μM,

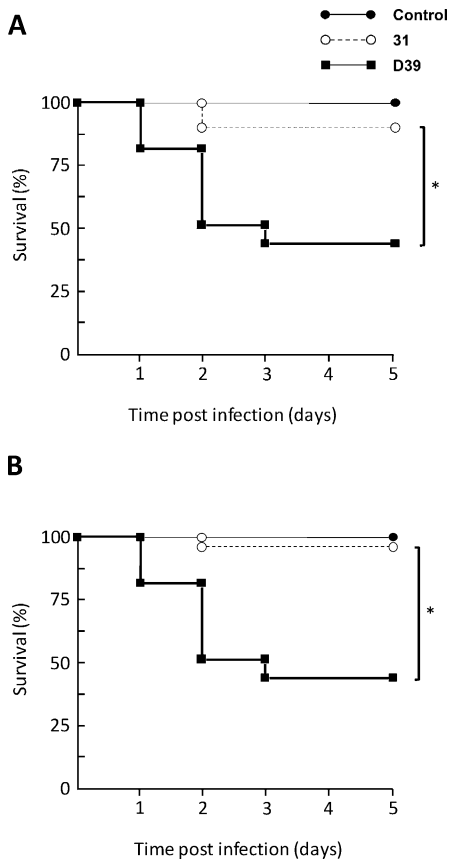

Figure 2. Rescue of zebrafish embryos from pneumococcal infection by **31**. Survival of embryos infected with 2.5×10^8 cfu mL^{-1} of *S. pneumoniae* D39 strain and treated with three doses of 1 μM (A) or 2 μM (B) of **31** ($n=24$ to 36 embryos per condition) is shown. Embryos were monitored for survival over a period of 5 days and results were plotted as Kaplan–Meier survival curves. Survival curves were compared with the log-rank (Mantel–Cox) and Gehan–Breslow–Wilcoxon tests (*, $P<0.001$).

comparable to usual β-lactam, macrolide, and fluoroquinolone antibiotics (1–12 μM).[12] Nevertheless, we aimed to further diminish EBA functional concentrations by increasing their affinity for CBPs through their multivalent display on poly(propylene imine) dendrimers. Previously, we found that choline dendrimers inhibit CBP activity more efficiently than free choline, but without affecting cell viability.[6a,7] To transform this non-lethal response into a more aggressive one, and as a proof-of-concept, we synthetized a second generation PPI dendrimer, termed g2-dendropine (Scheme 1b), containing eight copies of **2b**, a derivative of phenylacetyltropine (**2**) containing a five-carbon spacer (Supporting Information, Scheme S1). Phenylacetyltropine is a hydroxymethyl-lacking atropine analogue that displays only a modest C-LytA-GFP binding (Supporting Information, Figure S1). Since the 3-OH group in atropine does not participate in CBP binding,[8] this position seemed suitable to hold a five-carbon link for the attachment to the PPI scaffold. Moreover, phenylacetyltropine binds to the muscarinic acetylcholine receptors with diminished affinity compared to atropine, so that its antimuscarinic activity is drastically reduced to a mere 0.3 %,[13] decreasing undesirable side-effects in an eventual therapeutic administration of this or related dendrimers.

Compound **2b** binds to C-LytA with a lower apparent affinity than atropine and is inefficient in causing cell lysis at a 1 mM concentration (Supporting Information, Figures S2a and S5a), probably because of steric hindrances by the carbon spacer. Nevertheless, multicopy display of **2b** on the PPI dendrimer greatly enhances its apparent binding affinity to C-LytA-GFP (Supporting Information, Figure S7) as well as its LytA inhibitory efficiency in vitro, with an IC_{50} in the nanomolar range (Table 2), that is, around 45000-fold lower than atropine.[5b] Despite atropine being a better CBP binder than choline,[5b] the IC_{50} of g2-dendropine (100 nM) (Table 2) is similar to that of the previously described choline dendrimer g2-cho (200 nM), marking the limit of multivalency effects of this system. However, while g2-cho only induces chain formation without affecting cell viability,[6,7] a concentration of g2-dendropine as low as 1 μM (8 μM in atropine equivalents) is sufficient to completely abolish growth of the R6 strain, while cellular viability is negligible at 10 μM (Figure 3).

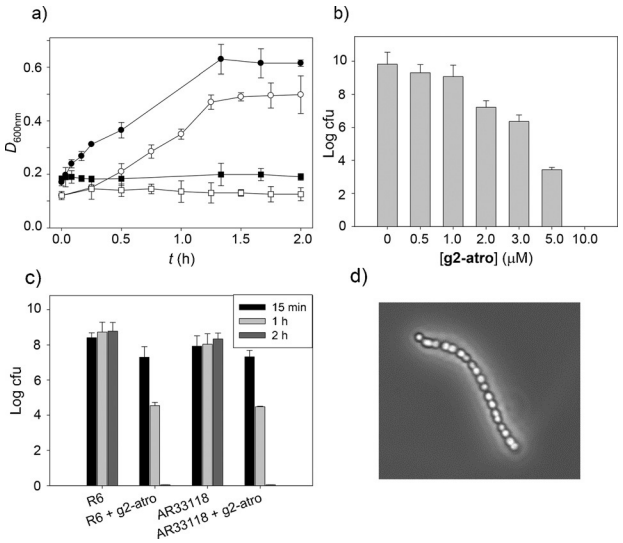

Figure 3. Effect of g2-dendropine on pneumococcal growth. a) Attenuation of liquid cultures of R6 (closed symbols) and AR33118 (open symbols) strains, in the absence (circles) or in the presence (squares) of g2-dendropine 1 μM (R6) or 10 μM (AR33118) (the minimal concentrations that arrest growth). Results are the average of duplicates. b) Dependence of R6 cell viability on g2-dendropine concentration (cfu: colony forming units). c) Effect on cell viability of incubation time with 10 μM g2-dendropine. d) Phase-contrast micrographs of AR33118 taken 15 min after being challenged with 50 μM g2-dendropine.

Furthermore, g2-dendropine was able to arrest the growth of a highly pathogenic, levofloxacin-resistant, pneumococcal clinical isolate (strain AR33118, serotype 3), albeit at a higher concentration (10 μM) (Figure 3a,b). To check the kinetics of this antimicrobial effect, cell viability was assessed upon challenge with 10 μM g2-dendropine for different times. An incubation as short as 15 min is enough to decrease viability by 10-fold, both for R6 and AR33118, and after 2 h virtually all cells became non-viable (Figure 3c). Likewise, clear

morphological changes are quickly visible, resulting in a "white" phenotype (Figure 3d) similar to that described above for **31** (Figure 1b; Supporting Information, Figure S4).

In conclusion, we have demonstrated the validity of two complementary approaches to design new antipneumococcal drugs targeting the bacterial CBPs. The best results were observed with tertiary amine EBAs with at least two non-heterocyclic, aromatic rings. A dramatic enhancement in apparent affinity can also be achieved by the display of EBAs on a multivalent dendrimer. Judicious combination of further EBA derivatives with multivalent nanoparticles may render novel complexes with antipneumococcal properties that help fight current resistances to antibiotics.

Acknowledgements

This work was supported by grants BFU2010-17824 and BIO2013-47684-R (Spanish Ministry of Education and Science), and EU-CP223111 (CAREPNEUMO, European Union). We thank M. Gutiérrez and J. Casanova for excellent technical assistance.

Keywords: antibiotic resistance · choline-binding proteins · dendrimers · drug design · pneumococcus

How to cite: *Angew. Chem. Int. Ed.* **2015**, *54*, 13673–13677
Angew. Chem. **2015**, *127*, 13877–13881

[1] a) World Health Organization. *Antimicrobial Resistance: Global Report on Surveillance* **2014**; b) K. Bush et al., *Nat. Rev. Microbiol.* **2011**, *9*, 894–896; c) M. McCarthy, *Br. Med. J.* **2013**, *347*, f5649.

[2] a) K. L. O'Brien, L. J. Wolfson, J. P. Watt, E. Henckle, M. Deloria-Knoll, N. McCall, E. Lee, K. Mulholland, O. S. Levine, T. Cherian, *Lancet* **2009**, *374*, 893–902; b) WHO. *Weekly Epidemiol. Rec.* **2007**, *82*, 93–104.

[3] a) S. Bergmann, S. Hammerschmidt, *Microbiology* **2006**, *152*, 295–303; b) M. J. Jedrzejas, *Cell. Mol. Life Sci.* **2007**, *64*, 2799–2822; c) P. García, M. Moscoso, V. Rodríguez-Cerrato, J. Yuste, E. García, *J. Appl. Biomed.* **2010**, *8*, 131–140.

[4] a) E. García, R. López, *FEMS Microbiol. Rev.* **2004**, *28*, 553–580; b) I. Pérez-Dorado, S. Galán-Bartual, J. A. Hermoso, *Mol. Oral Microbiol.* **2012**, *27*, 221–245.

[5] a) J. M. Sanz, R. López, J. L. García, *FEBS Lett.* **1988**, *232*, 308–312; b) B. Maestro, A. González, P. García, J. M. Sanz, *FEBS J.* **2007**, *274*, 364–376.

[6] a) V. M. Hernández-Rocamora, B. Maestro, B. de Waal, M. Morales, P. García, E. W. Meijer, M. Merkx, J. M. Sanz, *Angew. Chem. Int. Ed.* **2009**, *48*, 948–951; *Angew. Chem.* **2009**, *121*, 966–969; b) V. M. Hernández-Rocamora, S. W. A. Reulen, B. de Waal, E. W. Meijer, J. M. Sanz, M. Merkx, *Chem. Commun.* **2011**, *47*, 5997–5999.

[7] S. Ribes, J. Riegelmann, S. Redlich, B. Maestro, B. de Waal, E. W. Meijer, J. M. Sanz, R. Nau, *Chemotherapy* **2013**, *59*, 138–142.

[8] N. Silva-Martín, M. G. Retamosa, B. Maestro, S. G. Bartual, M. J. Rodes, P. García, J. M. Sanz, J. A. Hermoso, *Biochim. Biophys. Acta Gen. Subj.* **2014**, *1840*, 129–135.

[9] J. M. Sanz, B. Maestro, *Biochem. J.* **2005**, *387*, 479–488.

[10] E. G. Hohenstein, C. D. Sherrill, *J. Phys. Chem. A* **2009**, *113*, 878–886.

[11] R. Díez-Martínez, H. D. de Paz, N. Bustamante, E. García, M. Menéndez, P. García, *Antimicrob. Agents Chemother.* **2013**, *57*, 5355–5365.

[12] B. A. Cunha, P. E. Schoch, E. J. Bottone in *Antibiotic Essentials* (Ed.: B. A. Cunha), Jones and Bartlett Publishers LLC, Sudbury MA, USA, **2009**.

[13] a) S. D. C. Ward, C. A. M. Curtis, E. C. Hulme, *Mol. Pharmacol.* **1999**, *56*, 1031–1041; b) L. Gyermek, *Pharmacology of Anti-muscarinic Agents*, CRC, Boc Raton, **1997**, p. 173.

Received: June 20, 2015
Revised: July 30, 2015
Published online: September 17, 2015

